J|A|C|S ARTICLES

Published on Web 11/04/2009

Rational Design of d-PeT Phenylethynylated-Carbazole Monoboronic Acid Fluorescent Sensors for the Selective Detection of α-Hydroxyl Carboxylic Acids and Monosaccharides

Xin Zhang,[†] Lina Chi,[†] Shaomin Ji,[†] Yubo Wu,[†] Peng Song,[‡] Keli Han,[‡] Huimin Guo,[§] Tony D. James,[||] and Jianzhang Zhao*,[†]

State Key Laboratory of Fine Chemicals, School of Chemical Engineering, P.O. Box 40, 158 Zhongshan Road, Dalian University of Technology, Dalian 116012, P. R. China, State Key Laboratory of Molecular Reaction Dynamics, Dalian Institute of Chemical Physics, Chinese Academy of Sciences, 457 Zhongshan Road, Dalian 116023, P. R. China, Department of Chemistry, School of Chemical Engineering, Dalian University of Technology, Dalian 116012, P. R. China, and Department of Chemistry, University of Bath, Bath BA2 7AY, United Kingdom

Received July 20, 2009; E-mail: zhaojzh@dlut.edu.cn

Abstract: We have synthesized three new phenylethynylated carbazole boronic acid sensors, which were predicted to display novel d-PeT fluorescence transduction (PeT, photoinduced electron transfer; fluorophore as the electron donor of the electron transfer, ET) by DFT/TDDFT calculations. The d-PeT effect is characterized by a lower background fluorescence at acidic pH than at neutral pH, which is in stark contrast to the normal a-PeT effect (fluorophore as the electron acceptor of the ET) that shows a strong and undesired background fluorescence at acidic pH. Our experimental results confirmed the theoretical predictions and d-PeT was observed for two of the sensors (with *p*-dimethylaminophenylethynyl substitution at 6- position of the carbazole core). For the third sensor (with phenylethynyl substitution at 6- position of the carbazole core), however, not d-PeT but rather the normal a-PeT was observed. The discrepancy between the DFT/TDDFT calculations and the experimental observations can be rationalized using free energy changes (Rehm−Weller equations) and the rate constants for the ET (k_{ET}, Marcus equation). These new d-PeT boronic acid sensors show improved photophysical properties compared to the known d-PeT sensor reported previously by us. In particular, the fluorescence transduction efficiency of the new sensors was improved 8-fold when compared to the known d-PeT boronic acid sensors. Novel fluorescence enhancement/reduction was observed for one of the sensors upon binding with mandelic acid or tartaric acid at pH 5.6. The effect of pH as well as the bonding with analytes on the emission of the sensors were rationalized using DFT/TDDFT calculations. We believe that rational sensor design aided by DFT/TDDFT calculations as well as using free energy changes and electron transfer rate constants to study the emission properties of PeT sensors will become an essential tool in the design of new fluorophores or fluorescent sensors with predetermined photophysical properties.

1. Introduction

Fluorescent molecular sensors have attracted much attention due to their versatile applications in environmental, biological, and chemical science.[1−9] However, the rational design of fluorescent molecular sensors with predetermined photophysical properties still represents a significant challenge. The three key components for the successful design of fluorescent sensors are an appropriate fluorophore, binding unit, and sensing mechanism.[3,10] Popular fluorescence transduction mechanisms are based on manipulation of electron transfer (ET), for example, photoinduced electron transfer (PeT),[3,11] intramolecular charge transfer (ICT), etc.[5,6,12−17] For PeT sensors, a nitrogen atom usually

[†] State Key Laboratory of Fine Chemicals, Dalian University of Technology.
[‡] State Key Laboratory of Molecular Reaction Dynamics, Dalian Institute of Chemical Physics.
[§] Department of Chemistry, Dalian University of Technology.
[||] Department of Chemistry, University of Bath, UK.

(1) Lakowicz, J. R. *Principles of Fluorescence Spectroscopy*, 2nd ed.; Kluwer Academic: New York, 1999.
(2) Valeur, B. *Molecular Fluorescence: Principles and Applications*; Wiley-VCH Verlag GmbH: New York, 2001.
(3) De Silva, A. P.; Gunaratne, H. Q. N.; Gunnlaugsson, T.; Huxley, A. J. M.; McCoy, C. P.; Rademacher, J. T.; Rice, T. E. *Chem. Rev.* **1997**, *97*, 1515–1566.
(4) Pu, L. *Chem. Rev.* **2004**, *104*, 1687–1716.
(5) James, T. D. *Top. Curr. Chem.* **2007**, *277*, 107–152.
(6) Mohr, G. J. *Anal. Bioanal. Chem.* **2006**, *386*, 1201–1214.
(7) Gonçalves, M. S. T. *Chem. Rev.* **2009**, *109*, 190–212.
(8) Caltagirone, C.; Gale, P. A. *Chem. Soc. Rev.* **2009**, *38*, 520–563.
(9) Oshovsky, G. V.; Reinhoudt, D. N.; Verboom, W. *Angew. Chem., Int. Ed.* **2007**, *46*, 2366–2393.
(10) Ji, S.; Yang, J.; Yang, Q.; Liu, S.; Chen, M.; Zhao, J. *J. Org. Chem.* **2009**, *74*, 4855–4865.
(11) Kavarnos, G.; Turro, N. J. *Chem. Rev.* **1986**, *86*, 401–449.
(12) Stibor, I.; Zlatuskova, P. *Top. Curr. Chem.* **2005**, *255*, 31–63.
(13) Pu, L. *Chem. Rev.* **1998**, *98*, 2405–2494.
(14) Lin, J.; Pu, L. *Angew. Chem., Int. Ed.* **2005**, *44*, 1690–1693.

 10.1021/ja9060646 CCC: $40.75

acts as the fluorescence switch, then chelation with analytes fixes the otherwise transferable electrons. In this case, a specific pH range is required to optimize the fluorescence transduction of the PeT, since protonation of the *N* atom (at acidic pH) will increase the background emission of the sensor and this will substantially reduce the sensitivity of the fluorescence sensing.[3,5,18−22] Thus, neutral or basic pH are required for most of the a-PeT sensors (fluorophore as the acceptor of ET) to function efficiently.

Recently we have embarked on a study of boronic acid sensors,[17,18,23−29] which are unique because covalent bonds, instead of hydrogen bonds, are formed in molecular recognition. As a result, the recognition of analytes with boronic acid sensors can be carried out in aqueous media.[5,28,30−54] During our investigations, we discovered that these a-PeT boronic acid sensors do not work well in the acidic pH region.[5,18,54] Some analytes, however, such as α-hydroxylcarboxylic acids (mandelic acid, etc), require recognition at acidic pH, where the binding is much stronger than that at neutral or basic pH.[5,17,18,24,54] Unfortunately, the known a-PeT boronic acid sensors can not address this problem; therefore, a new sensing mechanism is required, ideally producing a better signal at acidic pH. Furthermore, many fluorescent molecular sensors are usually prepared using a trial and error approach, rather than using a rational design strategy. Although the trial and error approach has generated some good systems, a rational design of fluorescent chemosensors with predetermined photophysical properties is more desirable.[10]

Recently, we found that carbazole-based boronic acid sensor **4** shows d-PeT effect (fluorophore as the donor of the ET) (Scheme 1); with this system, the fluorescence emission intensity is decreased at acidic pH relative to neutral pH.[27] Recognition of tartaric acid with sensor **4** was observed at pH 4.0, where the binding is much stronger than that at neutral and basic pH. This kind of d-PeT sensor is rarely reported,[22] and this efficient fluorescence transduction at acidic pH upon binding was not observed for the normal a-PeT sensors.[18] However, the excitation/emission wavelength of sensor **4** was short (332 nm/372 nm) and the Stokes shift was also small (40 nm), reducing the potential applicability for measurement of biological samples. Furthermore, the PeT fluorescence transduction efficiency of the sensor **4** was low, for example, the emission intensity increased by only 0.25-fold when the pH was switched from acidic to basic.[27] In stark contrast, the normal a-PeT sensors show up to 10-fold fluorescence enhancement on switching the pH from basic to acidic.[18] Therefore, the performance of the d-PeT boronic acid sensor **4** needed to be improved. More importantly, the d-PeT mechanism required detailed investigation, to determine the relationship between molecular structure and the d-PeT effect to aid future sensor design.

Herein we report our results for the d-PeT boronic acid sensors **1**−**3** with phenylethynylated carbazole as the fluorophore (Scheme 1). The D-π-A feature of the sensors was varied to tune the PeT efficiency, through the introduction of electron-donating or electron-withdrawing groups. DFT/TDDFT calculations were then carried out prior to the synthesis of these sensors to verify the anticipated d-PeT effect. These sensors show red-shifted emission as well as larger Stokes shifts compared to the reported d-PeT sensor **4** (Scheme 1).[27] More importantly, the new d-PeT sensor demonstrated substantially improved

(15) Gunnlaughsson, T.; Glynn, M.; Tocci, G. M.; Kruger, P. E.; Pfeffer, F. M. *Coord. Chem. Rev.* **2006**, *250*, 3094–3117.
(16) Mader, H. S.; Wolfbeis, O. S. *Microchim. Acta.* **2008**, *162*, 1–34.
(17) Zhao, J.; Fyles, T. M.; James, T. D. *Angew. Chem., Int. Ed.* **2004**, *43*, 3461–3464.
(18) Zhao, J.; Davidson, M. G.; Mahon, M. F.; Kociok-Kohn, G.; James, T. D. *J. Am. Chem. Soc.* **2004**, *126*, 16179–16186.
(19) McCarroll, M. E.; Shi, Y.; Harris, S.; Puli, S.; Kimaru, I.; Xu, R.; Wang, L.; Dyer, D. J. *J. Phys. Chem. B.* **2006**, *110*, 22991–22994.
(20) Sunahara, H.; Urano, Y.; Kojima, H.; Nagano, T. *J. Am. Chem. Soc.* **2007**, *129*, 5597–5604.
(21) Cody, J.; Mandal, S.; Yang, L.; Fahrni, C. J. *J. Am. Chem. Soc.* **2008**, *130*, 13023–13032.
(22) (a) Ueno, T.; Urano, Y.; Setsukinai, K.; Takakusa, H.; Kojima, H.; Kikuchi, K.; Ohkubo, K.; Fukuzumi, S.; Nagano, T. *J. Am. Chem. Soc.* **2004**, *126*, 14079–14085. (b) Matsumoto, T.; Urano, Y.; Shoda, T.; Kojima, H.; Nagano, T. *Org. Lett.* **2007**, *9*, 3375–3377.
(23) Zhao, J.; James, T. D. *J. Mater. Chem.* **2005**, *15*, 2896–2901.
(24) Zhao, J.; James, T. D. *Chem. Commun.* **2005**, 1889–1891.
(25) Liang, X.; James, T. D.; Zhao, J. *Tetrahedron* **2008**, *64*, 1309–1315.
(26) Chi, L.; Zhao, J.; James, T. D. *J. Org. Chem.* **2008**, *73*, 4684–4687.
(27) Han, F.; Chi, L.; Liang, X.; Ji, S.; Liu, S.; Zhou, F.; Wu, Y.; Han, K.; Zhao, J.; James, T. D. *J. Org. Chem.* **2009**, *74*, 1333–1336.
(28) Nonaka, A.; Horie, S.; James, T. D.; Kubo, Y. *Org. Biomol. Chem.* **2008**, *6*, 3621–3625.
(29) Scrafton, D. K.; Taylor, J. E.; Mahon, M. F.; Fossey, J. S.; James, T. D. *J. Org. Chem.* **2008**, *73*, 2871–2874.
(30) Fujita, N.; Shinkai, S.; James, T. D. *Chem. Asian J.* **2008**, *3*, 1076–1091.
(31) Heinrichs, G.; Schellentraeger, M.; Kubik, S. *Eur. J. Org. Chem.* **2006**, *18*, 4177–4186.
(32) Levonis, S. M.; Kiefel, M. J.; Houston, T. A. *Chem. Commun.* **2009**, 2278–2280.
(33) Roy, D.; Cambre, J. N.; Sumerlin, B. S. *Chem. Commun.* **2009**, 2106–2108.
(34) Zhang, L.; Kerszulis, J. A.; Clark, R. J.; Ye, T.; Zhu, L. *Chem. Commun.* **2009**, 2151–2153.
(35) Cao, H.; McGill, T.; Heagy, M. D. *J. Org. Chem.* **2004**, *69*, 2959–2966.
(36) DiCesare, N.; Adhikari, D. P.; Heynekamp, J. J.; Heagy, M. D.; Lakowicz, J. R. *J. Fluoresc.* **2002**, *12*, 147–154.
(37) Jin, S.; Li, M.; Zhu, C.; Tran, V.; Wang, B. *ChemBioChem.* **2008**, *9*, 1431–1438.
(38) Wang, J.; Jin, S.; Akay, S.; Wang, B. *Eur. J. Org. Chem.* **2007**, 2091–2099.
(39) Powell, M. E.; Kelly, A. M.; Bull, S. D.; James, T. D. *Tetrahedron Lett.* **2009**, *50*, 876–879.
(40) Halo, T. L.; Appelbaum, J.; Hobert, E. M.; Balkin, D. M.; Schepartz, A. *J. Am. Chem. Soc.* **2009**, *131*, 438–439.
(41) Lim, S. H.; Musto, C. J.; Park, E.; Zhong, W.; Suslick, K. S. *Org. Lett.* **2008**, *10*, 4405–4408.
(42) Cao, H. S.; Diaz, D. I.; DiCesare, N.; Lakowicz, J. R.; Heagy, M. D. *Org. Lett.* **2002**, *4*, 1503–1505.
(43) Lavigne, J. J.; Anslyn, E. V. *Angew. Chem., Int. Ed.* **1999**, *38*, 3666–3669.
(44) Zhu, L.; Zhong, Z.; Anslyn, E. V. *J. Am. Chem. Soc.* **2005**, *127*, 4260–4269.
(45) Gao, X.; Zhang, Y.; Wang, B. *Tetrahedron.* **2005**, *61*, 9111–9117.
(46) Jin, S.; Zhu, C.; Li, M.; Wang, B. *Bioorg. Med. Chem. Lett.* **2009**, *19*, 1596–1599.
(47) (a) Zhu, L.; Shabbir, S. H.; Gray, M.; Lynch, V. M.; Sorey, S.; Anslyn, E. V. *J. Am. Chem. Soc.* **2006**, *128*, 1222–1232. (b) Wright, A. T.; Anslyn, E. V. *Chem. Soc. Rev.* **2006**, *35*, 14–28.
(48) Trupp, S.; Schweitzer, A.; Mohr, G. J. *Org. Biomol. Chem.* **2006**, *4*, 2965–2968.
(49) Kim, Y.; Hilderbrand, S. A.; Weissleder, R.; Tung, C. *Chem. Commun.* **2007**, 2299–2301.
(50) Yang, X. P.; Lee, M. C.; Sartain, F.; Pan, X. H.; Lowe, C. R. *Chem.—Eur. J.* **2006**, *12*, 8491–8497.
(51) Dowlut, M.; Hall, D. G. *J. Am. Chem. Soc.* **2006**, *128*, 4226–4227.
(52) Jiang, S.; Escobedo, J. O.; Kim, K. K.; Alpturk, O.; Samoei, G. K.; Fakayode, S. O.; Warner, I. M.; Rusin, O.; Strongin, R. M. *J. Am. Chem. Soc.* **2006**, *128*, 12221–12228.
(53) Wang, Z.; Zhang, D.; Zhu, D. *J. Org. Chem.* **2005**, *70*, 5729–5732.
(54) James, T. D.; Samankumara Sandanayake, K. R. A.; Iguchi, R.; Shinkai, S. *J. Am. Chem. Soc.* **1995**, *117*, 8982–8987. (b) Arimori, S.; Bell, M. L.; Oh, C. S.; Frimata, K. A.; James, T. D. *Chem. Commun.* **2001**, 1836–1837. (c) Arimori, S.; Bell, M. L.; Oh, C. S.; Frimat, K. A.; James, T. D. *J. Chem. Soc., Perkin Trans. 1* **2002**, 803–808. (d) Katif, N.; Harries, R. A.; Kelly, A. M.; Fossey, J. S.; James, T. D.; Marken, F. *J. Solid State Electrochem.* **2009**, *13*, 1475–1482. (e) Bromba, C.; Carrie, P.; Chui, J. K. W.; Fyles, T. M. *Supramol. Chem.* **2009**, *21*, 81–88.

Scheme 1. Synthesis of the Fluorescent Boronic Acid Sensors **1**−**3**[a]

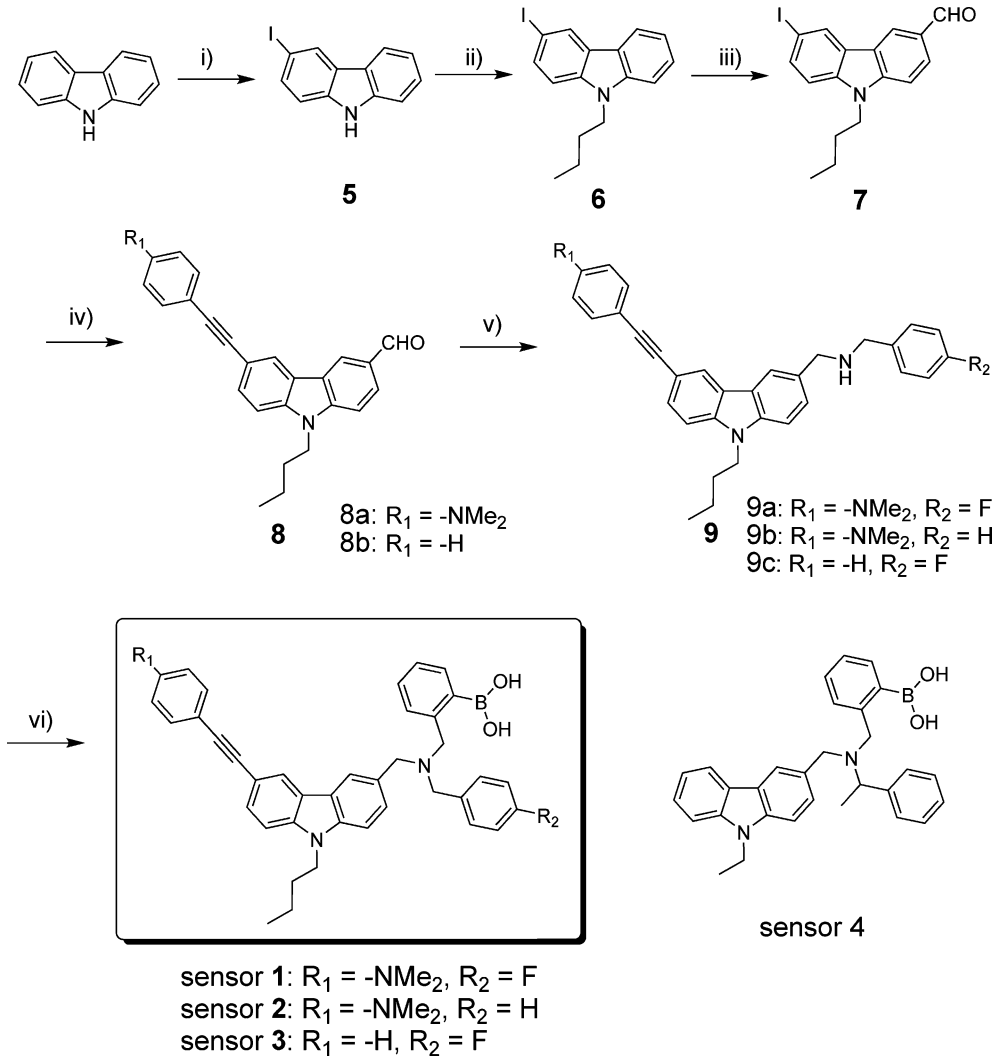

[a] Reported d-PeT boronic acid sensor **4** is also shown. (i) KI, KIO_3, CH_3COOH, reflux, 10 min, 45%; (ii) NaH, DMF, *n*-C_4H_9Br, room temperature, 1 h, 72%; (iii) $POCl_3$, DMF, CH_2Cl_2, reflux, 8 h, 63%; (iv) $Pd(PPh_3)_4$, CuI, NEt_3, 4-ethynyl-*N*,*N*-dimethylaniline or phenylacetylene, argon atmosphere, 60 °C, 8 h, 83−90%; (v) ethanol, THF, 4-fluorobenzylamine or benzylamine, reflux, 6 h, then methanol, THF, $NaBH_4$, room temperature, 15 min; (vi) acetonitrile, K_2CO_3, 2-(2-bromomethylphenyl)-1,3,2-dioxaborinane, reflux, 10 h, 15−35%.

fluorescence transduction efficiency, compared to a previous d-PeT boronic acid sensor reported by us.[27] Rich fluorescence transductions were found for sensor **1** toward recognition of hydroxyl acids and monosaccharides. For example, fluorescence enhancement/reduction was found for sensor **1** with tartaric acid/mandelic acid at pH 5.6. To our knowledge, this is a new fluorescence transduction profile and such chemoselectivity can be beneficial in the design of new analytical methods.[17] Interestingly, sensor **3** was found to be a normal a-PeT sensor, not the d-PeT sensor predicted by DFT/TDDFT calculations. We found that the discrepancy between the theoretical predictions and experimental observations can be rationalized by consideration of the free energy changes of the ET ($\Delta G°$, by Rehm−Weller equation) and the rate constants of ET (k_{ET}, by Marcus equation). The large fluorescence transductions of these sensors and the effect of structural modification on the PeT effect coupling with DFT/TDDFT calculation-aided sensor design will be of great interest for the future design of fluorescent sensors or fluorophores with predetermined photophysical properties.

2. Results and Discussion

2.1. Rational Design of d-PeT Fluorescent Sensors with Predetermined Photophysical Properties. To investigate the d-PeT fluorescence transduction mechanism in detail and to improve the performance of the carbazole-based d-PeT boronic acid sensor **4** reported by us,[27] sensors **1**−**3** were designed. Desired improvements include longer excitation/emission wavelengths, larger Stokes shifts, and more importantly improved fluorescence transduction efficiencies, for example, enhanced emission intensity on switching the pH from acidic to neutral (Scheme 1).[27] The π-conjugation framework of the sensors was extended by attaching phenylethynyl groups to the parent carbazole fluorophore. The electron-donating group (-NMe_2) was attached at the para position of alkynyl unit. 4-Fluorobenzylamine was also used to strengthen the electron-accepting capability of the boronic acid/amine moiety.[21]

We have shown that the fluorescence transduction of the d-PeT effect can be rationalized with DFT/TDDFT calculations.[27] Thus, the photophysical properties of the designed sensors were investigated by DFT/TDDFT calculations prior

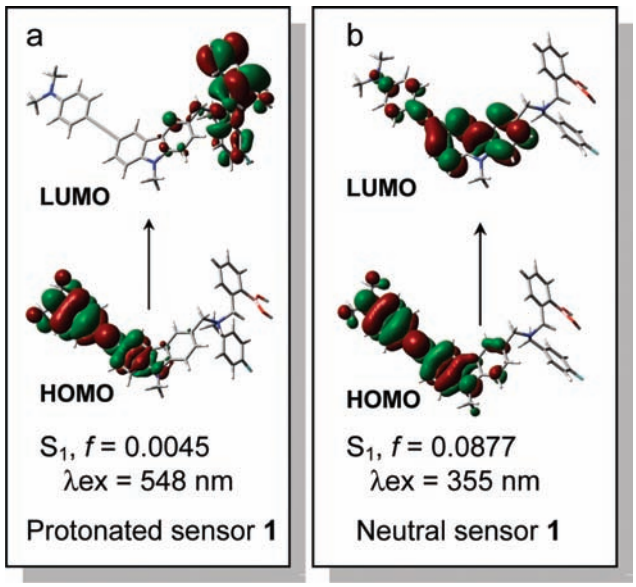

Figure 1. Prediction of the d-PeT effect for sensor **1** by DFT/TDDFT calculations. (a) Main transitions of the singlet excited state of the protonated sensor **1**. $S_1 \leftarrow S_0$ (LUMO←HOMO. $f = 0.0045$). S_1 is a dark state (no emission or weakly emissive), with ICT character. (b) Main transitions of the singlet excited state of the neutral sensor **1**, $S_1 \leftarrow S_0$ (LUMO←HOMO. $f = 0.0877$). $S_1 \leftarrow S_0$ of neutral sensor **1** is an allowed electronic transition (potentially emissive), and S_1 can be recognized as a LE state.

to the synthesis of these sensors. The optimized structures of the sensors show that the phenylethynyl and the carbazole moieties are in coplanar geometry, inferring that π-conjugation between the carbazole core and the peripheral phenylalkynyl moiety will be efficient; thus, we expect a red-shifted emission wavelength for sensor **1**.[55,56] The HOMO−LUMO distributions of the S_1 state of sensor **1** are presented in Figure 1. The main electronic transitions of sensor **1** (either the neutral form or the monoprotonated form of the sensor) are compiled in Table 1.

The evaluation of the electronic excited states and the photophysical properties of the sensor are based on the selection rule for electronic transitions.[2,10,27,57] A transition can be considered as forbidden if there is no overlap between the initial and the destination MOs involved in the transition (e.g., S_1 of the protonated sensor **1**, Figure 1a). Another parameter to evaluate the possibility of a transition is the oscillator strength (f). Usually transitions with $f > 0.01$ are allowed; conversely, a small $f < 0.01$ infers a forbidden transition ($f = 0.01$ corresponding to extinction coefficient, ε, ca. 1000 cm^{-1} mol^{-1} dm^3).[58] The same rules are applicable to the emission processes.[2,10,57,58]

ET from the arylalkynyl moiety to boronic acid moiety was observed for the S_1 state of the protonated sensor **1** (protonation at the alkylamine, Figure 1a, see also Scheme 2), with $f = 0.0045$ (excitation energy of 548 nm). The small f value and the lack of overlap between the HOMO and the LUMO makes the transition moment very small, thus $S_1 \leftarrow S_0$ is a forbidden transition and the S_1 state can not be directly populated by photoexcitation but will be populated by internal conversion (IC) from higher excited states, such as the S_8 state.[2,10,57,58] Thus, S_1 is not an emissive state; it is a dark state.[10,27,58] This means no radiative decay will occur; instead, nonradiative decay will act as the drain pipe for the energy of the excited state. Therefore, we propose that the protonated probe **1** will be weakly fluorescent. A low-lying allowed excited state of S_8 shows $f = 0.9759$ (340 nm), which is in good agreement with the UV−vis absorption at 360 nm (Table 2), thus validating the theoretical calculations.

In contrast to the protonated **1**, the S_1 state of the neutral sensor **1** is a locally excited state (LE, Figure 1b). Furthermore, the oscillator strength (f) is 0.0877, about 20 times higher than that of the protonated sensor **1**. This means the neutral sensor **1** will probably fluorescence stronger than the protonated sensor **1**. The calculated excitation energy of the S_1 state is 355 nm, which is in good agreement with the experimental results (360 nm, Table 2).

On the basis of these calculations, we conclude that the protonated sensor **1** will give weaker emission than the neutral sensor **1**, that is, sensor **1** is a d-PeT sensor, in that the emission intensity-pH profile is reversed when compared to the normal PeT effect (a-PeT). We have demonstrated that the d-PeT effect is complementary to the normal a-PeT effect,[27] that is, the α-hydroxyl acids can be recognized with higher fluorescence transduction efficiency at acidic pH, where the binding is stronger than that at neutral or basic pH.[17,18,24]

To interpret the theoretical calculations for the d-PeT effect more intuitively, we calculated the fluorescence lifetimes of the sensors, the Einstein transition probabilities of the spontaneous transitions, which are described by eq 1.[10,59]

$$\tau = \frac{c^3}{2(E)^2 f} \tag{1}$$

where τ is the fluorescence lifetime, c stands for the light velocity, E is the transition energy, and f is the oscillator strength (Table 1). All of the parameters are in atomic unit (au). The calculated fluorescence lifetimes for the protonated sensor **1** and the neutral sensor **1** are 1002 and 21 ns, respectively. The reasonable lifetime of the neutral sensor **1** (21 ns) infers that it is probably fluorescent. For the protonated probe **1**, however, the exceptionally long lifetimes are far beyond the τ range for relaxation of a singlet excited state (the emissive state for most organic fluorophores),[1,2] which leads to nonradiative decay of the excited state. These results indicate that the protonated probe **1** will be nonfluorescent or weakly fluorescent.

The low-lying excited states of **2** and **3** were also examined using similar considerations. d-PeT effects were predicted for these sensors (see Figures S76−S79 and Tables S2, S3 in Supporting Information). To validate our theoretical predictions, we subsequently synthesized sensors **1**−**3**. Experimental results confirmed that sensors **1** and **2** are d-PeT sensors, as predicted by the DFT/TDDFT calculations. However, experimentally, sensor **3** is a-PeT sensor, and not the theoretically predicted d-PeT sensor. The discrepancy between the theoretical calculations and the experimental observations for sensor **3** can be

(55) Adhikari, R. M.; Neckers, D. C.; Shah, B. K. *J. Org. Chem.* **2009**, *74*, 3341–3349.
(56) Xing, J.; Chen, W.; Gu, J.; Dong, X.; Takeyasu, N.; Tanaka, T.; Duan, X.; Kawata, S. *J. Mater. Chem.* **2007**, *17*, 1433–1438.
(57) Parson, W. W. *Modern Optical Spectroscopy: With Examples from Biophysics and Biochemistry*; Springer-Verlag: Berlin Heidelberg, 2007.
(58) (a) Zhao, G.; Liu, J.; Zhou, L.; Han, K. *J. Phys. Chem. B.* **2007**, *111*, 8940–8945. (b) Saita, K.; Nakazono, M.; Zaitsu, K.; Nanbo, S.; Sekiya, H. *J. Phys. Chem. B.* **2009**, *113*, 8213–8220.
(59) Liu, Y.; Feng, J.; Ren, A. *J. Phys. Chem. A* **2008**, *112*, 3157–3164.

Table 1. Selected Electronic Excitation Energies (eV) and Oscillator Strengths (*f*), Configurations of the Low-Lying Excited States of the Neutral Sensor **1** and the Monoprotonated Sensor **1** ($[1 + H]^+$)[a]

		TDDFT//B3LYP/6-31G(d)			
	electronic transition	energy (eV)[b]	*f*[c]	composition[d]	CI[e]
1	$S_0 \rightarrow S_1$	3.49 (355 nm)	0.0877	H→L	0.6381
				H→L+1	0.2114
	$S_0 \rightarrow S_2$	3.68 (336 nm)	1.4546	H→L+1	0.6202
	$S_0 \rightarrow S_3$	3.94 (314 nm)	0.0025	H→L+2	0.7052
	$S_0 \rightarrow S_4$	4.14 (299 nm)	0.0087	H→L+3	0.7052
$[\mathbf{1}+\mathbf{H}]^+$	$S_0 \rightarrow S_1$	2.26 (548 nm)	0.0045	H →L	0.7027
	$S_0 \rightarrow S_2$	2.47 (502 nm)	0.0401	H→ L+1	0.6627
				H→ L+2	0.2165
	$S_0 \rightarrow S_6$	3.10 (400 nm)	0.3586	H→ L+5	0.6869
	$S_0 \rightarrow S_8$	3.64 (340 nm)	0.9759	H→ L+6	0.6390
	$S_0 \rightarrow S_{12}$	4.08 (303 nm)	0.0563	H−3→L	0.5841
				H−1→L+3	0.3477

[a] Calculated by TDDFT//B3LYP/6-31G(d), based on the optimized ground state geometries. [b] Only selected excited states were considered. The numbers in parentheses are the excitation energy in wavelength. [c] Oscillator strength. [d] H stands for HOMO and L stands for LUMO. Only the main configurations are presented (CI coefficients >0.2). [e] CI coefficients are in absolute values.

Scheme 2. Simplified Fluorescence Transduction Mechanisms of Sensor **1**[a]

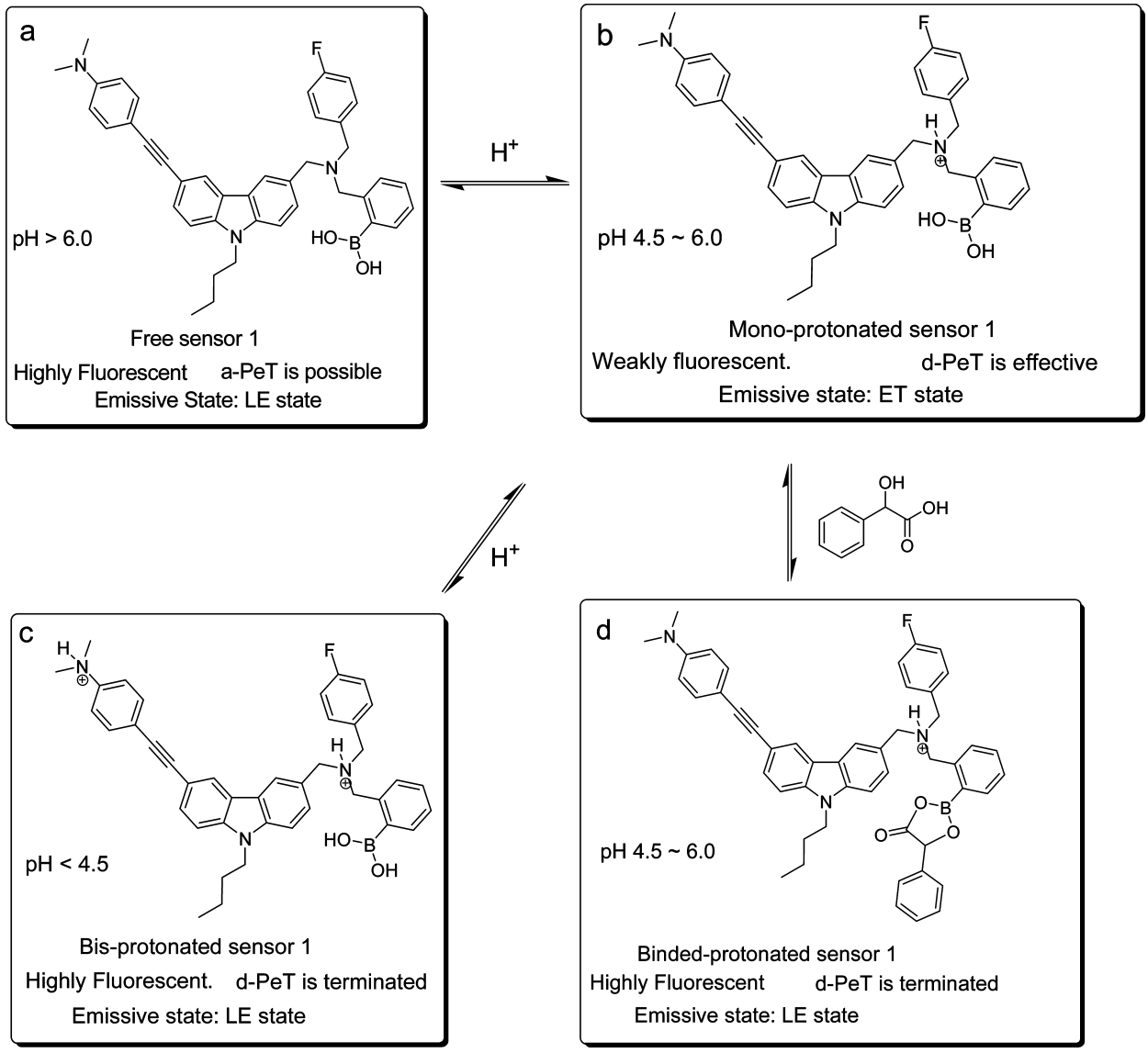

[a] (a) Free sensor **1** in media with pH > 6.0, is highly fluorescent. (b) Monoprotonated sensor **1** (weakly fluorescent, in media with pH 4.5−6.0). (c) Bis-protonated species (in media with pH < 4.5, highly fluorescent). (d) Analyte bonded species (a-PeT is terminated). These assumptions are based on the experimental results (vide infra) and were supported by DFT/TDDFT calculations.

Table 2. Photophysical Parameters of Sensors **1**−**4**

	ε (M^{-1} cm^{-1}) [a]	λ_{abs} (nm)	λ_{em} (nm)	Stokes shift/(nm)	Φ[b](pH 4.0)	Φ [b](pH7.5)	τ (ns) [c]	k_r [d] ($\times$ 10^7 s^{-1})	k_{nr} [e] ($\times$ 10^7 s^{-1})
sensor **1**	2.83×10^4	360	430	70	0.04	0.06	5.23	1.22	17.9
sensor **2**	4.88×10^4	370	450	80	0.07	0.12	4.77	2.57	18.3
sensor **3**	2.96×10^4	338	393	55	0.44	0.21	6.80	3.07	11.6
sensor **4**	4.69×10^4	332	372	40	0.24	0.31	7.02	4.43	9.8

[a] In 5.0×10^{-2} mol dm^{-3} NaCl ionic buffer (52.1% methanol in water), pH 7.5. [b] Fluorescence quantum yields, with quinine sulfate as the standard ($\Phi = 0.54$ in 0.5 M H_2SO_4). [c] Fluorescence lifetimes, with typical error of 0.01 ns. Concentrations of the sensors are 3.0×10^{-5} mol dm^{-3}. [d] Radiative decay rate constants at pH 7.5, $k_r = \Phi/\tau$. [e] Nonradiative decay rate constants at pH 7.5, $k_{nr} = (1-\Phi)/\tau$.

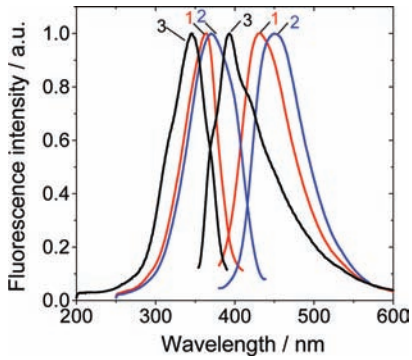

Figure 2. Normalized excitation and emission spectrum of sensors **1**−**3**; 3.21×10^{-6} mol dm^{-3} of sensors in 5.0×10^{-2} mol dm^{-3} NaCl ionic buffer (52.1% methanol in water), pH 7.4. For sensor **1**: $\lambda_{ex} = 360$ nm, $\lambda_{em} = 430$ nm; for sensor **2**: $\lambda_{ex} = 370$ nm, $\lambda_{em} = 450$ nm; for sensor **3**: $\lambda_{ex} = 340$ nm, $\lambda_{em} = 393$ nm; 18 °C.

rationalized by consideration of the free energy changes and the rate constants of the ET (vide infra).

2.2. Synthesis of the Alkynyl Carbazole Fluorescent Boronic Acid Sensors. The design rationale of sensors **1**−**3** lies in the notion that carbazole acts as the fluorophore;[60,61] the phenylethynyl groups were introduced to increase the π-conjugation and thus the excitation/emission wavelength. Electron-donating (Me_2N-) and electron-withdrawing units (F atom) were used to tune the d-PeT efficiencies.[56,62,63] First the carbazole moiety was monoiododied,[64] then **5** was butylated in the presence of NaH.[65] 3-Formalated compound **7** was obtained with the Vilsmeier reaction. The π-conjugation frameworks of the sensors were extended with Sonogashira cross-coupling to obtain fluorophores with emission at a longer wavelength than the parent fluorophore (sensor **4**, Scheme 1). Then with reductive amination and reaction with 2-(2-bromomethylphenyl)-1,3,2-dioxaborinane, the monoboronic acid sensors **1**−**3** were obtained. All of the compounds were obtained in satisfying yields (14−35%).

2.3. Excitation/Emission Spectra of the Sensors and Observation of the Predicted d-PeT Effect. The fluorescence spectra of probes **1**−**3** were recorded (Figure 2). The excitation/emission bands of sensors **1**−**2** are structureless, compared to the structured excitation/emission spectra of the previous d-PeT sensor,[27] clearly indicating that electronic communication is efficient between the moieties at both ends of the ethynylene group for sensors **1** and **2**.[56,62,63] This observation is supported by the theoretical calculations. The emission of **1** is centered at 430 nm, which is red-shifted by 58 nm compared to the emission of the known d-PeT boronic acid sensor.[27] Another key photophysical parameter, the Stokes shift, increased to 70 from 40 nm when compared with the known d-PeT sensor.[27] A large Stokes shift is beneficial for potential fluorescent molecular sensing, especially fluorescent bioimaging.[10,66−68] The excitation/emission wavelengths of sensor **2** are red-shifted compared to those of sensor **1**. The structure difference of **1** and **2** is F substitution in sensor **1** but not in sensor **2**. The electron-withdrawing F atom is not directly attached to fluorophore so we did not expect it to disturb the excitation/emission wavelength profoundly. We attribute this spectral change to the different polarity of the microenvironment in which the fluorophore resides,[69] for example, the perturbation of the π-conjugation system by the F atom. We noticed that the pK_a of sensor **2** is 5.11 ± 0.05 (see Supporting Information), which is different from the pK_a of sensor **1** (4.79 ± 0.14).

Sensor **3** lacks an electron-donating group (-NMe_2). The excitation/emission (338 nm/393 nm) of sensor **3** shows blue-shifts compared to that of sensors **1** and **2**. The Stokes shift of sensor **3** (55 nm) is also decreased compared to that of sensor **1** (70 nm) and sensor **2** (80 nm). Furthermore, structured excitation/emission bands were observed, which is in contrast to the structureless excitation/emission bands of sensors **1** and **2**. These results indicate that the photophysical properties of ethynylated carbazole can be tuned by electron-donating or electron-withdrawing substitutions, even at the 3,6-position of the carbazole moiety.[55]

To prove the predicted d-PeT effect of sensor **1**, the pH dependency of the emission of sensor **1** was studied (Figure 3). Three pH ranges with dramatic different emission intensity-pH response can be identified. From pH 11.23 to pH 6.37, the emission hardly shows any changes (see Figure S26 in Supporting Information). When the pH was decreased from 6.37 to 4.23, however, the emission intensity decreased (Figure 3a); this is in stark contrast to the normal a-PeT sensors.[3−5,18,24,25,70] The pK_a for the d-PeT effect was determined as 4.79 ± 0.14 (Figure 4). This abnormal pH-emission intensity profile clearly demonstrates the d-PeT effect and is in full agreement with the theoretical calculations (Table 1). The fluorescence intensity transduction of the new sensor is greatly improved compared to the previous d-PeT

(60) Galmiche, L.; Mentec, A.; Pondaven, A.; Her, M. L. *New J. Chem.* **2001**, *25*, 1148–1151.
(61) Velasco, D.; Castellanos, S.; Lopez, M.; Lopez-Calahorra, F.; Brillas, E.; Julia, L. *J. Org. Chem.* **2007**, *72*, 7523–7532.
(62) Jian, H.; Tour, J. M. *J. Org. Chem.* **2003**, *68*, 5091–5103.
(63) Zhu, Z.; Moore, J. S. *J. Org. Chem.* **2000**, *65*, 116–123.
(64) Tucker, S. H. *J. Chem. Soc.* **1926**, 546–553.
(65) Xu, T.; Lu, R.; Qiu, X.; Liu, X.; Xue, P.; Tan, C.; Bao, C.; Zhao, Y. *Eur. J. Org. Chem.* **2006**, 4014–4020.
(66) Zhou, Y.; Xiao, Y.; Chi, S.; Qian, X. *Org. Lett.* **2008**, *10*, 633–636.
(67) Peng, X.; Du, J.; Fan, J.; Wang, J.; Wu, Y.; Zhao, J.; Sun, S.; Xu, T. *J. Am. Chem. Soc.* **2007**, *129*, 1500–1501.
(68) Peng, X.; Song, F.; Lu, E.; Wang, Y.; Zhou, W.; Fan, J.; Gao, Y. *J. Am. Chem. Soc.* **2005**, *127*, 4170–4171.
(69) Jin, S.; Wang, J.; Li, M.; Wang, B. *Chem.—Eur. J.* **2008**, *14*, 2795–2804.
(70) Zheng, S.; Lin, N.; Reid, S; Wang, B. *Tetrahedron* **2007**, *63*, 5427–5436.

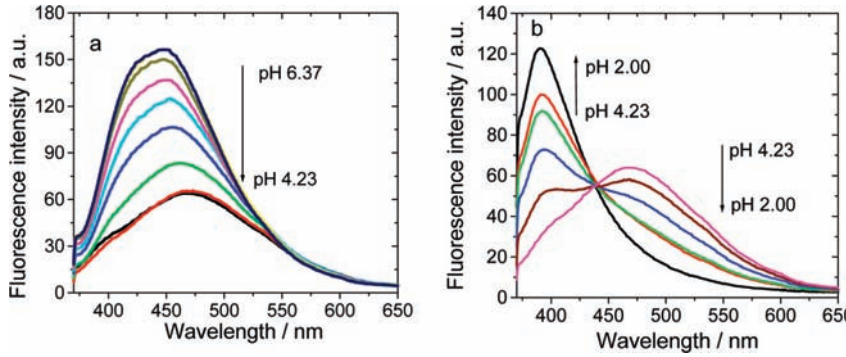

Figure 3. Fluorescence spectral changes of sensor **1** (3.21×10^{-6} mol dm^{-3}) at different pH; 5.0×10^{-2} mol dm^{-3} NaCl ionic buffer (52.1% methanol in water). (a) From pH 6.37 to 4.23; (b) from pH 4.23 to 2.00. $\lambda_{ex} = 360$ nm; 18 °C.

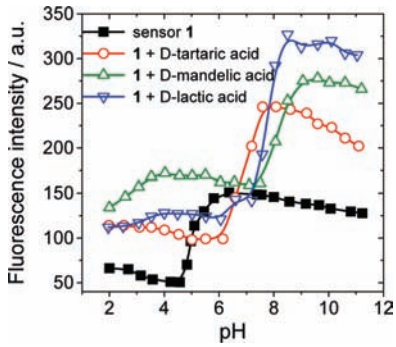

Figure 4. Fluorescence intensity-pH profile of probe **1** in the presence of D-tartaric acid, D-mandelic acid, and D-lactic acid. The concentration of hydroxyl acids is 2.5×10^{-2} mol dm^{-3}; 3.21×10^{-6} mol dm^{-3} of sensor **1** in 5.0×10^{-2} mol dm^{-3} NaCl ionic buffer (52.1% methanol in water). $\lambda_{ex} = 360$ nm, $\lambda_{em} = 430$ nm; 18 °C.

sensor.[27] For example, the fluorescence enhancement is ca. 2-fold for sensor **1**, on switching the pH from 4.23 to 6.37, while the reported d-PeT boronic sensor shows only a 0.25-fold enhancement.[27] We attribute this improvement to the stronger electron-donating ability of the modified fluorophore. By decreasing the pH from 4.23 to 2.00, a new emission band at 390 nm developed and the emission intensity at 475 nm concomitantly decreased (Figure 3b). The pK_a value for this change is 3.31 ± 0.10 (Figure 4). We propose that this pH-dependency of the emission at pH 2.0−4.5 is due to the switch from an ICT to LE emission state, caused by protonation of the dimethylaminophenyl moiety. With protonation of the aryl nitrogen atom (Scheme 2c), the ICT excited state will be replaced by a LE excited state.[3,10,71] At the same time the electron-donating capability of the phenylethynylene moieties decreased, so we also propose that the d-PeT is terminated at low pH, which enhances the fluorescence emission.

The above postulation about the fluorescence changes at pH 4.5−2.0, and the transition of the S_1 from ICT to LE state was also rationalized by DFT/TDDFT calculations (Figure S75 and Table S1 in Supporting Information). The *f* value for S_1 of the bis-protonated sensor **1** is as high as 1.0008 and indicates S_1 as an emissive state.[10,58] This is fully supported by experimental observations (Figure 3).

The emission intensity-pH profiles of probes **2** and **3** were also studied and d-PeT was found for probe **2** (see Figure S35 in Supporting Information). For probe **3**, however, the normal a-PeT effect was observed (see later discussion). We propose that the a-PeT effect for probe **3** is due to the lack of the electron donating group, -NMe_2. The d-PeT as well as the a-PeT effect of the sensors can be rationalized by considering the free energy changes of the sensors.[2,19−22,72] We noticed that sensors **1** and **2** show relatively strong emissions at basic pH; this is different from the normal a-PeT sensors.[18] Fluorescence quantum yields also support the analysis (Table 2). For example, sensor **1** gives Φ of 0.04 at pH 4.0 (protonated). Conversely, Φ = 0.06 was observed at pH 7.5. This is in contrast to sensor **3**, which show the a-PeT effect with reversed Φ profiles (Table 2).

2.4. pH and Analyte Titration of Sensor 1. The recognition of analytes by sensor **1** show rich fluorescence transduction motifs. The pH titration of sensor **1** with and without analytes is presented in Figure 4. In the presence of tartaric acid, the emission intensity of sensor **1** increased at pH 4.0 compared to the emission of blank sensor but decreased at pH 6.0 and increased again in the pH range 8−10 (Figure 4). Notably, the sensor gave large fluorescence enhancement at basic pH in the presence of tartaric acid and mandelic acid (for the binding curves, see Figure S28 and Figure S29 in Supporting Information); this is in stark contrast to the sensors with normal a-PeT effect.[18] Such a rich fluorescence transduction was not observed for normal PeT boronic sensors.[18,24,73−75] The apparent pK_a values of sensor **1** increased to 6.83 ± 0.11 ($r^2 = 0.9356$) in the presence of tartaric acid, from 4.79 ± 0.14.

Good chemoselectivity was found for sensor **1** toward the recognition of tartaric acid and mandelic acid. For example, at pH 5.6, the emission of the sensor decreased in the presence of tartaric acid but increased in the presence of mandelic acid (Figures 4 and 5). The mechanism for this enhancement/reduction is unclear.[27]

The emission spectra changes of sensor **1** in the presence of tartaric acid and mandelic acid at pH 4.0, 5.6, and 7.5 are presented in Figure 5. At pH 4.0, fluorescence enhancement was observed in the presence of either tartaric acid or mandelic acid (Figure 5a,d). Thus, the recognition of hydroxyl acid with significant fluorescence transduction was achieved at acidic pH with the d-PeT effect.[18,27]

At pH 5.6, the emission intensity decreased in the presence of tartaric acid but increased in the presence of mandelic

(71) Zhao, G.; Chen, R.; Sun, M.; Liu, J.; Li, G.; Gao, Y.; Han, K.; Yang, X.; Sun, L. *Chem.—Eur. J.* **2008**, *14*, 6935–6947.
(72) Mineno, T.; Ueno, T.; Urano, Y.; Kojima, H.; Nagano, T. *Org. Lett.* **2006**, *8*, 5963–5966.
(73) Kawanishi, T.; Romey, M. A.; Zhu, P. C.; Holody, M. Z.; Shinkai, S. *J. Fluoresc.* **2004**, *14*, 499–512.
(74) Phillips, M. D.; James, T. D. *J. Fluoresc.* **2004**, *14*, 549–559.
(75) Cao, H.; Heagy, M. D. *J. Fluoresc.* **2004**, *14*, 569–584.

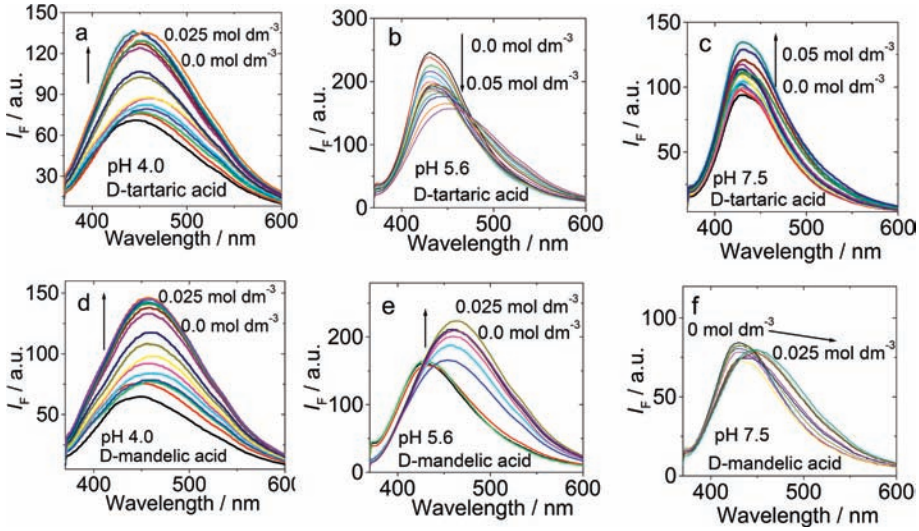

Figure 5. Emission spectra of sensor **1** in the presence of D-tartaric acid at (a) pH 4.0; (b) pH 5.6; (c) pH 7.5 and the emission spectra in the presence of D-mandelic acid at (d) pH 4.0; (e) pH 5.6; (f) pH 7.5. 3.21×10^{-6} mol dm^{-3} of sensor **1** in 5.0×10^{-2} mol dm^{-3} NaCl ionic buffer (52.1% methanol in water), 18 °C. $\lambda_{ex} = 360$ nm.

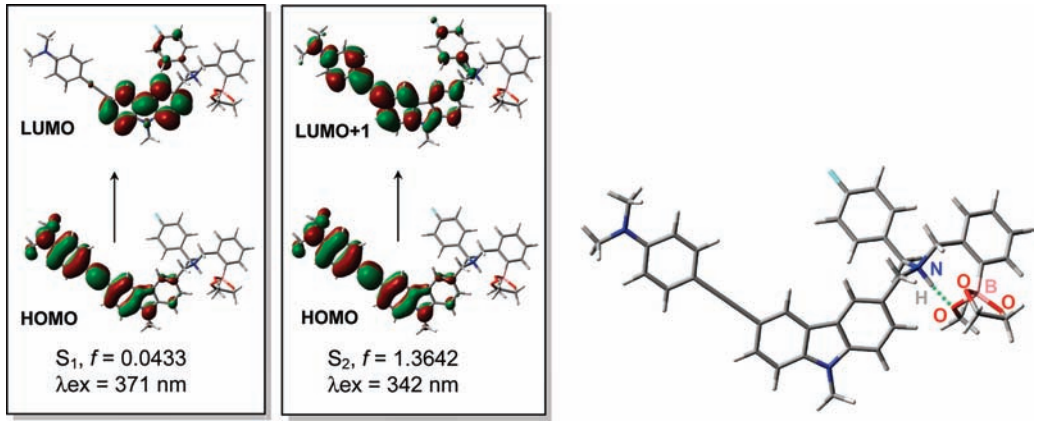

Figure 6. Termination of the d-PeT effect of the protonated sensor **1** upon binding with analyte (the analyte was simplified as ethylene glycol, $OHCH_2CH_2OH$, to reduce the calculation time (MeOH inserted zwitterionic structure). The transitions for the low-lying excited states of $S_1 \leftarrow S_0$ (LUMO←HOMO) and $S_2 \leftarrow S_0$ (LUMO+1←HOMO) are presented. Note $S_1 \leftarrow S_0$ is an allowed electronic transition with oscillator strength $f = 0.0433$. The optimized structure of the binding complex is shown.

acid (Figure 5). Moreover, red-shift of the emission peaks were observed in the presence of analytes; this observation is different from the normal a-PeT boronic acid sensors,[17,18,23,24] which show no shift of the emission band in the presence of analytes.

We propose that the fluorescence enhancement in the presence of tartaric acid at pH 4.0 is due to the transformation of boron from sp^2 to sp^3 hybridized, with release of the steric constrain caused by bonding with tartaric acid, and finally the termination of the d-PeT effect (quenching effect, see Scheme 2).

2.5. Rationalization of the Binding Induced Emission Enhancement at Acidic pH and the Solvent-Inserted Zwitterionic Structure of the Binding Complex. The above postulation on the enhancement of the emission of sensor **1** upon binding with analytes at acidic pH, that is, the fluorescence transduction mechanism with the d-PeT effect, can be rationalized using DFT/TDFFT calculations. The binding complex of **1** with analytes (simplified as ethylene glycol) was optimized, and the MOs of the low-lying electronic transitions of the complex are presented in Figure 6 and Table 3. It is accepted that upon bonding with an analyte, a solvent molecule inserted complex will result; that is, a methoxy group will bond to boron atom to release the steric strain, by transformation of sp^2 boron

Table 3. Selected Electronic Excitation Energies (eV) and Corresponding Oscillator Strengths (*f*), Main Configurations and CI Coefficients of the Low-Lying Electronically Excited States of Sensor **1** Bonded with Ethylene Glycol (see Figure 6 for the Structure of the Binding Complex)[a]

	TDDFT//B3LYP/6-31G(d)			
electronic transition	energy (eV)[b]	*f*[c]	composition[d]	CI[e]
$S_0 \rightarrow S_1$	3.34 (371 nm)	0.0433	H→L	0.6784
$S_0 \rightarrow S_2$	3.62 (342 nm)	1.3642	H→L+1	0.1984
$S_0 \rightarrow S_3$	3.75 (330 nm)	0.0015	H→L+2	0.6980
$S_0 \rightarrow S_4$	3.83 (323 nm)	0.1183	H→L+3	0.6941

[a] Methanol inserted zwitterionic structure was used for the calculation. Calculated by TDDFT//B3LYP/6-31G(d), based on the optimized ground state geometries. [b] Only selected low-lying excited states were considered. The numbers in parentheses are the excitation energy in wavelength. [c] Oscillator strength. [d] H stands for HOMO and L stands for LUMO. Only the main configurations are presented. [e] CI coefficients are in absolute values.

to sp^3 boron, and an intramolecular hydrogen bond will form.[18,28,34,41,47,52,76−81] It is only in aprotic solvents that the dative B−N will be formed.[5,47a,76]

A zwitterionic structure was used for the DFT calculations, and the boron atom takes a sp^3 tetrahedron geometry. The optimization displays an intramolecular hydrogen bond (H-bond) formed with the methoxy group as the H-bond acceptor and N−H as the H-bond donor. The optimized H-bond length (N−H···O) is 2.657 Å, which is very close to a crystal structure of boronate complex with a H-bond length (N−H···O) of 2.655 Å.[18,34,76] These results indicate that molecular optimization based on DFT calculations can precisely predict the geometries of the boronate complex.

On the basis of the optimized ground state geometries, we carried out the TDDFT calculation on the low-lying electronically excited states of the complex (Table 3). The oscillator strength of the S_1 state ($f = 0.0433$) of the complex increased by ca. 10-fold compared to that of the protonated sensor **1** ($f = 0.0045$, Figure 1 and Table 1). Moreover, there is overlap between the HOMO and LUMO (Figure 6).[10,58] Thus, we propose that the fluoresce of the complex may be intensified compared to the protonated sensor (free sensor **1**). These expectations based on the DFT/TDDFT calculations were verified by the experimental observations (Figure 5); that is, the emission of protonated sensor **1** intensified in the presence of analytes (Figure 5). Furthermore, we can see that the d-PeT effect of protonated sensor **1** (Figure 1) terminated upon binding an analyte. On the basis of the electronic transitions, we propose that the protonated amine/boronic acid groups act as ET acceptors and play an indispensable role for the d-PeT effect of protonated sensor **1**. The pH dependency of the compound without a boronic acid group, that is, amine **9a**, was also investigated and no d-PeT effect but rather the normal a-PeT effect was observed (see Figure S32 in Supporting Information).

2.6. Analyte Titration with the Sensors: Chemoselectivity through Emission Enhancement or Reduction. The binding curves of sensor **1** with mandelic acid and tartaric acid at pH 5.6 are presented in Figure 7. At pH 5.6, enhancement of the emission intensity was observed in the presence of mandelic acid, whereas the intensity was reduced in the presence of tartaric acid. Binding constants of $(3.20 \pm 0.28) \times 10^5$ M^{-1} and $(1.14 \pm 0.17) \times 10^4$ M^{-1} were determined for tartaric acid and mandelic acid, respectively. To our knowledge, chemoselectivity with enhancement/reduction of intensity in the presence of different analytes has never been reported for fluorescent chemosensors.[4,9,82,83]

The emission intensity of sensor **1** at pH 4.0 was enhanced in the presence of both tartaric acid and mandelic acid (see Figure S27 in Supporting Information). Binding constants of $(2.67 \pm 0.42) \times 10^4$ and $(3.99 \pm 0.84) \times 10^4$ M^{-1} were determined for tartaric acid and mandelic acid, respectively. Such a recognition ability at acidic pH is impossible for the normal a-PeT sensors, where the background emission of the sensor is too strong.[3,5,17,23,24]

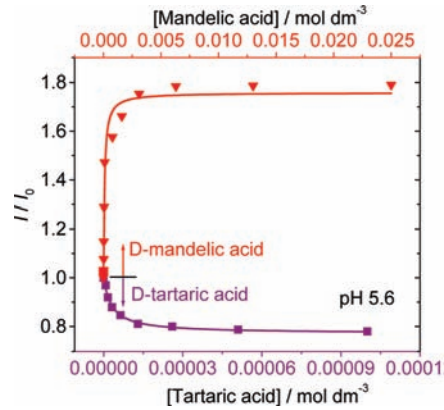

Figure 7. Relative fluorescence intensity of probe **1** vs concentrations of D-mandelic acid and tartaric acid at pH 5.6. For D-mandelic acid, $\lambda_{ex} = 360$ nm, $\lambda_{em} = 457$ nm. For d-tartaric acid, $\lambda_{ex} = 360$ nm, $\lambda_{em} = 454$ nm. The solid lines are the fitting results of 1:1 binding; 3.21×10^{-6} mol dm^{-3} of sensor **1** in 5.0×10^{-2} mol dm^{-3} NaCl ionic buffer (52.1% methanol in water), 18 °C.

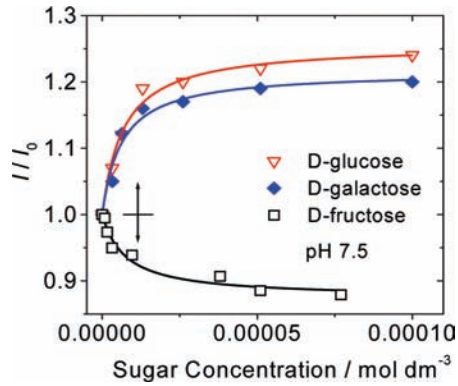

Figure 8. Binding isotherms of sensor **1** with monosaccharide at pH 7.5. The solid lines are the fitting results of 1:1 binding. $\lambda_{ex} = 360$ nm, $\lambda_{em} = 430$ nm; 3.21×10^{-6} mol dm^{-3} of sensor in 5.0×10^{-2} mol dm^{-3} NaCl ionic buffer (52.1% methanol in water); 18 °C.

The fluorescence transduction mechanisms for sensor **1** can be summarized in Scheme 2. The free sensor **1** (in media with pH > 6.0) is highly fluorescent. With monoprotonation of sensor **1**, the d-PeT effect was switched on; thus, the fluorescence intensity is reduced. On further reduction of the pH to pH < 4.0, the sensor became bis-protonated and the d-PeT effect was terminated (Figures 3 and 4); thus, the emission peak is blue-shifted and the intensity is enhanced. Upon binding with analytes, the d-PeT effect was also terminated; thus, fluorescence enhancement was observed (Figure 4). These assumptions are in agreement with the fluorescence measurement and are supported by the DFT/TDDFT calculations.

The emission intensity-pH profile of sensor **1** in the presence of glucose, fructose, and galactose were also investigated (Figure 8). Sensor **1** showed reduced emission in the presence of fructose at pH 7.5. But fluorescence enhancements were observed in the presence of glucose and galactose at pH 7.5. Binding constants of $(1.52 \pm 0.33) \times 10^5$ and $(1.28 \pm 0.53) \times 10^5$ M^{-1} were determined for glucose and fructose, respectively. The binding constant was $(1.70 \pm 0.50) \times 10^5$ M^{-1} for galactose. To our knowledge, recognition of monosaccharides with such fluores-

(76) Collins, B. E.; Sorey, S.; Hargrove, A. E.; Shabbir, S. H.; Lynch, V. M.; Anslyn, E. V. *J. Org. Chem.* **2009**, *74*, 4055–4060.
(77) Kaiser, P. F.; White, J. M.; Hutton, C. A. *J. Am. Chem. Soc.* **2008**, *130*, 16450–16451.
(78) Sartain, F. K.; Yang, X.; Lowe, C. R. *Chem.—Eur. J.* **2008**, *14*, 4060–4067.
(79) Gamsey, S.; Miller, A.; Olmstead, M. M.; Beavers, C. M.; Hirayama, L. C.; Pradhan, S.; Wessling, R. A.; Singaram, B. *J. Am. Chem. Soc.* **2007**, *129*, 1278–1286.
(80) Berube, M.; Dowlut, M.; Hall, D. G. *J. Org. Chem.* **2008**, *73*, 6471–6479.
(81) Kano, N.; Yoshino, J.; Kawashima, T. *Org. Lett.* **2005**, *7*, 3909–3911.
(82) Bell, T. W.; Hext, N. M. *Chem. Soc. Rev.* **2004**, *33*, 589–598.
(83) Lin, J.; Hu, Q.; Xu, M.; Pu, L. *J. Am. Chem. Soc.* **2002**, *124*, 2088–2089.

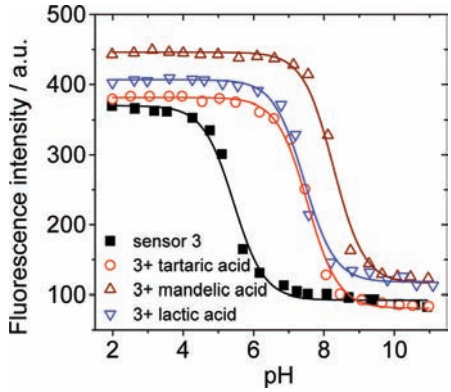

Figure 9. Fluorescence emission intensity-pH profile of sensor **3** with and without analytes. The solid lines are the pK_a fitting results of pH-intensity curves. The concentration of hydroxyl acids is 1.25×10^{-2} mol dm^{-3}; 3.0×10^{-6} mol dm^{-3} of sensor **3** in 5.0×10^{-2} mol dm^{-3} NaCl ionic buffer (52.1% methanol in water). $\lambda_{ex} = 340$ nm, $\lambda_{em} = 389$ nm; 18 °C.

cence enhancement/reduction has never been reported.[5,6,46,48,52,84] Such a phenomenon is rare, because boronic acid based sensors usually display fructose selectivity over other monosaccharides.

The emission intensity-pH profile of sensor **2** was also investigated, and the response in the presence of analytes, such as tartaric acid and mandelic acid, etc., was determined. It was found that sensor **2** is a d-PeT sensor (see Figure S34 in Supporting Information). However, the fluorescence transduction is relatively simple compared to that of sensor **1**. No fluorescence enhancement/reduction was observed in the presence of different analytes (see Figure S40, S42 and S44 in Supporting Information).

2.7. Normal PeT Effect of Sensor 3. Sensor **3** was designed without the electron-donating group (-NMe_2). d-PeT effect was predicted by DFT/TDDFT calculations (see Figures S78 and S79 and Table S3 in Supporting Information). The fluorescence emission spectra of sensor **3** as a function of the pH or in the presence of analytes was investigated. Interestingly, a normal a-PeT emission intensity-pH profile was observed, that is, sensor **3** show intensified emission at acidic pH and reduced emission at basic pH, with pK_a values of 5.43 ± 0.05 (Figure 9). This emission intensity-pH profile is typical for a-PeT system.

In the presence of tartaric acid, mandelic acid, and lactic acid, the emission intensity of sensor **3** was enhanced in the pH range 6.0−8.0, with apparent pK_a values of 7.53 ± 0.03, 8.28 ± 0.05, and 7.44 ± 0.05, respectively. This emission intensity-pH profile of the sensor alone or the sensor in the presence of analytes were similar to the normal a-PeT sensors.[18] Herein we can clearly see that the normal a-PeT mechanism is in operation. The recognition of tartaric acid or mandelic acid at pH 4.0 is impossible for sensor **3**, because the fluorescence enhancement in the presence of analytes is too small.[85−89] But with d-PeT sensor, that is, sensor **1**, the recognition of mandelic acid/tartaric acid at pH 4.0 was possible (Figures 4 and 5). The binding constants of the sensors with selected analytes of α-hydroxyl carboxylic acid and monosaccharide are compiled in Table 4.

Above all, sensor **1** and **2** are found to be d-PeT sensors, which is consistent with theoretical predictions. However, experimentally sensor **3** is a normal a-PeT effect system in disagreement with the theoretical predictions. We also demonstrated that the fluorescence transductions of the sensors in the presence of analytes are good (Figures 4, 5, 7, and 8).

2.8. Evaluate the d-PeT Effect Using Thermodynamics and Kinetics: Application of the Rehm−Weller and the Marcus Equations. To explain the discrepancy between the theoretically predicted d-PeT effect by DFT/TDDFT calculations and the experimentally observed a-PeT effect for sensor **3** (Figure 9), we used a thermodynamic criteria to evaluate the possibility of the electron transfer process, that is, the free energy changes ($\Delta G°$) of the d-PeT effect. This driving force for the ET can be obtained by using the Rehm−Weller equation (eq 2).[1,2,11,19−22]

$$\Delta G^\circ = E^\circ(D^+/D) - E^\circ(A/A^-) - \Delta E_{0,0} + w_p$$
$$w_p = \frac{e^2}{4\pi\varepsilon R} \qquad (2)$$

where $E°(D^+/D)$ is the oxidation potential of the electron donor, $E°(A/A^-)$ is the reduction potential of the electron acceptor; herein, the values are approximated as the energy difference of HOMO and LUMO (calculated with DFT). $\Delta E_{0,0}$ is the zero−zero transition energy (approximated as the crossing point of the excitation and the emission spectra of the sensors). ϵ is the dielectric constant of media (approximated as methanol with ϵ value of 32.7). R is the distance between the donor and acceptor (distance between the two N atoms of the carbazole and amine moieties, respectively, calculated by the DFT optimization).

Negative $\Delta G°$ means the ET is thermodynamically possible. Conversely, positive $\Delta G°$ value means the ET is impossible. Free energy changes for the ET of sensor **1** were calculated as $\Delta G° = -49.0$ kJ mol^{-1} (Table 5). For sensor **2**, $\Delta G° = -28.8$ kJ mol^{-1}. These negative values infer that ET may occur for sensor **1** and sensor **2**. Experimentally, d-PeT effect was observed for both sensor **1** and sensor **2** (Figure 4 and Supporting Information).

Similar consideration was also applied for sensor **3**, for which d-PeT effect was also predicted by DFT/TDDFT calculations (see Figure S77, Figure S78, and Table S3 in Supporting Information), but not observed experimentally (Figure 9). For sensor **3**, a positive free energy change of $\Delta G° = 14.5$ kJ mol^{-1} was obtained (Table 5), which infers that the ET can not occur spontaneously.[19] Thus the $\Delta G°$ values can be used to predict the d-PeT effect.

Alternatively, the effect of d-PeT on the emission profile of the sensors can also be evaluated by kinetics of the ET process of the ET effect. The kinetics of the ET is important because the two major competing process, the ET (quenching effect) and the radiative decay of the excited molecules (giving emission) dictate the fate of the excited states.[1−3] With the free energy changes of the ET (Table 5), the ET rate constants (k_{ET}) can be estimated by the Marcus equation (eq 3).[2,19,21]

$$k_{ET} = \left(\frac{4\pi^3}{\hbar^2 \lambda k_B T}\right)^{1/2} V^2 \exp\left[-\frac{(\Delta G^\circ + \lambda)^2}{4\lambda k_B T}\right] \qquad (3)$$

(84) James, T. D.; Shinkai, S. *Top. Curr. Chem.* **2002**, *218*, 159–200.
(85) Schertzer, B. M.; Baker, S. N.; Diver, S. T.; Baker, G. A. *Aust. J. Chem.* **2006**, *59*, 633–639.
(86) Tan, W.; Zhang, D.; Wang, Z.; Liu, C.; Zhu, D. *J. Mater. Chem.* **2007**, *17*, 1964–1968.
(87) Yu, Y.; Zhang, D.; Tan, W.; Wang, Z.; Zhu, D. *Bioorg. Med. Chem. Lett.* **2007**, *17*, 94–96.
(88) DiCesare, N.; Lakowicz, J. R. *Chem. Commun.* **2001**, 2022–2023.
(89) Luvino, D.; Gasparutto, D.; Reynaud, S.; Smietana, M.; Vasseur, J. *Tetrahedron Lett.* **2008**, *49*, 6075–6078.

Table 4. Stability Constants (M^{-1}) of Sensors **1**−**3** with α-Hydroxyl Acid and Monosaccharides

stability constants	pH	sensor **1**	sensor **2**	sensor **3**
tartaric acid	4.0	$(2.67 \pm 0.42) \times 10^4$	$(1.81 \pm 0.59) \times 10^4$	− [c]
	5.6	$(3.20 \pm 0.28) \times 10^5$	$(3.98 \pm 0.49) \times 10^4$	$(4.20 \pm 0.51) \times 10^3$ [b]
	7.5	$(1.74 \pm 0.93) \times 10^3$	$(1.49 \pm 0.27) \times 10^5$	− [c]
mandelic acid	4.0	$(3.99 \pm 0.84) \times 10^4$	$(4.28 \pm 1.01) \times 10^4$	− [c]
	5.6	$(1.14 \pm 0.17) \times 10^4$	$(1.22 \pm 0.16) \times 10^4$	$(1.58 \pm 0.16) \times 10^4$ [b]
	7.5	$(2.28 \pm 1.78) \times 10^3$	$(5.46 \pm 2.44) \times 10^3$	− [c]
lactic acid	4.0	$(4.33 \pm 0.56) \times 10^3$	$(3.31 \pm 1.06) \times 10^3$	− [c]
	5.6	$(6.47 \pm 1.62) \times 10^4$ [a]	$(5.28 \pm 0.11) \times 10^3$	$(4.16 \pm 0.41) \times 10^3$ [b]
	7.5	$(4.67 \pm 0.90) \times 10^4$	$(6.32 \pm 2.22) \times 10^4$	- [c]
glucose	7.5	$(1.52 \pm 0.33) \times 10^5$	$(6.56 \pm 1.68) \times 10^4$	$(1.33 \pm 0.28) \times 10^4$
galactose	7.5	$(1.70 \pm 0.50) \times 10^5$	$(2.33 \pm 0.89) \times 10^4$	$(2.56 \pm 0.73) \times 10^3$
fructose	7.5	$(1.28 \pm 0.53) \times 10^5$	$(1.73 \pm 0.62) \times 10^4$	$(4.36 \pm 0.84) \times 10^3$

[a] Fluorescence intensity decreased in the presence of analytes. [b] pH 6.0. [c] At which pH is not appropriate for binding constant determination.

Table 5. Parameters Used in the Calculation of the Free Energy Changes of the Potential d-PeT Effect With Rehm−Weller Equation (eq 2)[a]

	E_{HOMO}/(eV) [b]	E_{LUMO}/(eV) [b]	ΔE/(eV) [c]	$\Delta E_{0,0}$(eV) [d]	w_p(eV)	ΔG/kJ mol^{-1}/(eV)
sensor **1**	−6.18	−3.67	2.50	3.16	0.15	−49.0(−0.51)
sensor **2**	−6.15	−3.62	2.53	2.98	0.15	−28.8(−0.30)
sensor **3**	−7.13	−3.76	3.37	3.38	0.15	+14.5(+0.15)

[a] MeOH as the Solvent. [b] Calculated values. [c] $\Delta E = E_{LUMO} - E_{HOMO}$. [d] Crossing point of the excitation and emission spectra.

where $\hbar$ is Planck's constant, k_B is the Boltzmann constant, T is the absolute temperature, λ is the reorganization energy, and V is the electronic coupling matrix element. On the basis of the assumption that the radii of the donor moiety is about 5 Å, the radii of the ET acceptor is 2.5 Å (DFT optimization value), the λ values of the sensor **1** was calculated as 2.4 eV. The electronic coupling matrix of the three sensors molecules was arbitrarily assumed as 0.5 eV.[19] The k_{ET} values of the protonated sensors **1**, **2**, and **3** were calculated as 1.20×10^9 s^{-1}, 4.69×10^7 s^{-1}, and 7.37×10^4 s^{-1}, respectively ($k_{ET}^{max} = 2.71 \times 10^{15}$ s^{-1}). The ET rate constants of sensors **1** and **2** are comparable to the rate constants of radiative decay (fluorescence rate constant, k_r on scale of 10^7 s^{-1}, Table 1);[1,2] thus, the ET can compete with radiative decay, the fluorescence will be reduced, and this is the d-PeT effect. For the protonated sensor **3**, however, the extremely slow ET rate constants ($k_{ET} = 7.37 \times 10^4$ s^{-1}) implies that it cannot compete efficiently with the radiative decay process ($k_r = 3.07 \times 10^7$ s^{-1}); thus, fluorescence is possible and a-PeT effect is expected for sensor **3**. These considerations are in agreement with the experimental observations. It should be pointed out that these considerations are approximations because some of the parameters are estimated. However, the results clearly demonstrate the trend of the kinetics of the ET process for protonated sensors **1**−**3** and it is useful for evaluation of the photophysical properties of the sensors from a kinetic point of view.

Herein we have demonstrated the potential, as well as the limitations of the DFT/TDDFT calculation in the rational PeT sensor design. Our result demonstrated that thermodynamics as well as kinetics are also useful for evaluation of the photophysical properties of the fluorescent sensors. These results will be helpful for future rational design of fluorescent sensors and fluorophores with predetermined photophysical properties.

2.9. Conclusions. In conclusion, we synthesized three new phenylethynylated carbazole boronic acid sensors **1**−**3**. The sensors were rationally designed using DFT/TDDFT calculations, which predicted a d-PeT effect for all the sensors. Experimental results proved the theoretical predictions of a d-PeT effect for sensor **1** and **2**. However, for sensor **3**, no d-PeT was observed; instead, the normal a-PeT effect was observed. This discrepancy between the DFT/TDDFT calculations can be rationalized by consideration of the kinetics and thermodynamics of the ET process, that is, by using the Marcus (k_{ET}) and Rehm−Weller equations (free energy changes, $\Delta G°$). The d-PeT boronic acid sensors **1** and **2** show improved photophysical properties compared to the reported sensor, such as red-shifted emission wavelength, larger Stokes shifts, and most importantly improved fluorescence transduction efficiency of the d-PeT effect. The fluorescence intensity of **1** and **2** can be modulated by ca. 2-fold compared to the reported value of 0.25-fold; thus, the fluorescence modulation is 8× more efficient for the new d-PeT sensors. Fluorescence transduction of analyte recognition was observed, for example, novel fluorescence enhancement/reduction was observed for sensor **1** in the presence of mandelic acid or tartaric acid at pH 5.6. The effect of pH as well as the bonding with analytes on the emission of the sensors was rationalized using DFT/TDDFT calculations. We believe our successful application of DFT/TDDFT calculations and the free energy change considerations in the rationalization of the photophysical properties of the sensors reported herein may inspire others in the quest for the rational design of fluorophores and sensors with predetermined photophysical properties.

3. Experimental Section

3.1. Analytical Measurements. NMR spectra were recorded on a Bruker 400 MHz spectrometer ($CDCl_3$ or $CDCl_3/CD_3OD$ as solvents, TMS as standard, $\delta = 0.00$ ppm). High resolution mass spectra (HRMS) were determined on a LC/Q-TOF MS system (UK). Melting points were measured on a XPR-300C microscopic instrument. Fluorescence spectra were measured on a F4500 (Hitachi) or a CRT 970 spectrofluorometer. Fluorescence lifetimes were measured with a Fluoromax-4 spectrofluorometer (Horiba Jobin Yvon). Absorption spectra were recorded on a Perkin-Elmer-Lambda-35 UV/vis spectrophotometer. A 0.05 M NaCl (52.1% methanol in water, w/w) ionic buffer was used in the experiment. All pH were measured using a Delta 320 Microprocessor pH meter (Mettler Toledo).

3.2. Synthesis of 2-[[[(*N*-Butyl-6-[4′-dimethylaminophenylethynyl]-9H-carbazol-3-yl)methyl]-[[4′-fluorophenylmethyl]amino]methyl]phenyl]boronic Acid (Sensor 1). 9a (100 mg, 0.20 mmol), 2-(2-bromomethylphenyl)-1,3,2-dioxaborinane (65.0 mg, 0.26 mmol), and K_2CO_3 (118.0 mg, 0.86 mmol) were mixed in acetonitrile (5 mL); the mixture was refluxed for 10 h under N_2. The mixture was cooled, and dichloromethane was added. The organic layer was washed with water and dried over anhydrous Na_2SO_4. The solvent was removed, and the residue was purified with column chromatography (Al_2O_3, ethyl acetate/MeOH, 100:1, V/V). Yellow powder (18.5 mg) was obtained, yield: 14.6%. Mp

169−171 °C. ^{1}H NMR (400 MHz, $CDCl_3/CD_3OD$) δ 8.26 (s, 1H), 7.94 (s, 1H), 7.85 (d, 1H, J = 6.0 Hz), 7.61 (d, 1H, J = 8.4 Hz), 7.45 (d, 2H, J = 8.8 Hz), 7.25−7.38 (m, 7H), 7.17 (d, 1H, J = 6.4 Hz), 7.02−7.06 (m, 2H), 6.69 (d, 2H, J = 8.8 Hz), 4.29 (t, 2H, J = 7.2 Hz), 3.79 (s, 2H), 3.77 (s, 2H), 3.60 (s, 2H), 3.00 (s, 6H), 1.82−1.88 (m, 2H), 1.38−1.43 (m, 2H), 0.96 (t, 3H, J = 7.6 Hz). ^{13}C NMR (100 MHz, $CDCl_3/CD_3OD$) δ 150.0, 141.8, 140.5, 140.1, 136.8, 132.7, 132.1, 131.7, 131.6, 131.5, 130.6, 129.5, 128.0, 127.7, 126.4, 123.8, 122.7, 122.6, 122.3, 115.6, 115.4, 114.5, 112.1, 110.9, 109.2, 108.9, 88.7, 88.6, 61.5, 57.9, 56.5, 43.2, 40.5, 31.3, 20.7, 14.0. ESI-HRMS ($[C_{41}H_{41}BFN_3O_2 + H]^+$) calcd 638.3354, found 638.3377.

3.3. Synthesis of 2-[[[(*N*-Butyl-6-[4′-dimethylaminophenylethynyl]-9H-carbazol-3-yl)methyl]-[[phenylmethyl]amino]methyl]phenyl]boronic Acid (Sensor 2). Similar procedure to the synthesis of sensor **1** was used. Yellow powder (27.1 mg) was obtained, yield: 21.3%. Mp 76−78 °C. ^{1}H NMR (400 MHz, $CDCl_3/CD_3OD$) δ 8.26 (s, 1H), 7.96 (s, 1H), 7.83 (d, 1H, J = 6.4 Hz), 7.61−7.63 (m, 1H), 7.45−7.47 (m, 2H), 7.28−7.39 (m, 10H), 7.19 (br, 1H), 6.70−6.72 (m, 2H), 4.30 (t, 2H, J = 7.2 Hz), 3.83 (s, 2H), 3.80 (s, 2H), 3.66 (s, 2H), 3.00 (s, 6H), 1.83−1.90 (m, 2H), 1.37−1.46 (m, 2H), 0.94 (t, 3H, J = 7.2 Hz). ^{13}C NMR (100 MHz, $CDCl_3/CD_3OD$) δ 150.1, 140.5, 140.2, 136.3, 132.7, 131.5, 131.4, 131.3, 130.1, 130.0, 129.4, 128.7, 128.6, 128.2, 127.8, 127.7, 127.5, 123.7, 122.7, 122.5, 122.4, 114.4, 112.2, 111.0, 109.0, 108.9, 88.6, 88.5, 61.2, 57.2, 56.6, 43.2, 40.4, 31.3, 20.7, 14.0. ESI-HRMS ($[C_{41}H_{42}BN_3O_2 + H]^+$) calcd 620.3448, found 620.3429.

3.4. Synthesis of 2-[[[(*N*-Butyl-6-[phenylethynyl]-9H-carbazol-3-yl)methyl]-[[4′-fluorophenylmethyl]amino]methyl]phenyl]-boronic Acid (Sensor 3). Similar procedure to the synthesis of sensor **1** was used. Yellow powder (45.8 mg) was obtained, yield: 34.9%. Mp 122−124 °C. ^{1}H NMR (400 MHz, $CDCl_3/CD_3OD$) δ 8.30 (s, 1H), 7.96 (s, 1H), 7.84 (d, 1H, J = 6.8 Hz), 7.64 (d, 1H, J = 7.6 Hz), 7.58 (d, 2H, J = 6.8 Hz), 7.26−7.40 (m, 11H), 7.02−7.06 (m, 2H), 4.31 (t, 2H, J = 7.2 Hz), 3.80 (s, 2H), 3.78 (s, 2H), 3.61 (s, 2H), 1.83−1.90 (m, 2H), 1.38−1.44 (m, 2H), 0.96 (t, 3H, J = 7.6 Hz).^{13}C NMR (100 MHz, $CDCl_3/CD_3OD$) δ 163.6, 161.2, 141.8, 140.6, 136.9, 132.2, 131.7, 131.6, 131.4, 130.5, 129.6, 128.5, 128.2, 128.0, 127.7, 126.6, 124.2, 124.1, 122.8, 122.6, 122.3, 115.6, 115.4, 113.6, 109.3, 109.0, 91.0, 87.8, 61.5, 58.0, 56.7, 43.3, 31.3, 20.7, 14.0. ESI-HRMS ($[C_{39}H_{36}BFN_2O_2 + H]^+$) calcd 595.2932, found 595.2913.

3.5. Computational Details. The ground state structures of sensors were optimized using density functional theory (DFT) with B3LYP functional and 6-31G (d) basis set. The excited state related calculations were carried out with the Time dependent DFT (TD-DFT) with the optimized structure of the ground state (DFT/6-31G(d). There are no imaginary frequencies in frequency analysis of all calculated structures; therefore, each calculated structures are in local an energy minimum. All of these calculations were performed with Gaussian 03.[90]

Acknowledgment. We thank the NSFC (20642003, 20634040, 20833008 and 40806042), Ministry of Education (SRF for ROCS, SRFDP-200801410004 and NCET-08-0077), PCSIRT(IRT0711), NKBRSF (2007CB815202), State Key Laboratory of Fine Chemicals (KF0710 and KF0802), State Key Laboratory of Chemo/Biosensing and Chemometrics (2008009), the Education Department of Liaoning Province (2009T015), and Dalian University of Technology (SFDUT07005 and 1000-893394) for financial support. T.D.J. and J.Z. are grateful to the Royal Society for fostering their collaboration through the China-UK Science Networks. The scheme has helped initiate annual Symposia and Joint Laboratories devoted to Catalysis & Sensing for our Environment (CASE). We are also grateful to the reviewers for their critical comments on the manuscript.

Supporting Information Available: General experimental methods, synthesis of compounds, compound characterization data (^{1}H NMR, ^{13}C NMR and HRMS), fluorescence spectra (emission intensity-pH profiles and binding curves) and DFT/TDDFT calculation details of sensors **1**−**3**. This material is available free of charge via the Internet at http://pubs.acs.org.

JA9060646

(90) Frisch, M. J.; et al. *Gaussian 03,* Revision D.01, Gaussian, Inc.: Wallingford, CT, 2003.